DNAJC14 rescues the pathology of misfolded pendrin

Hyeji Choi

Department of Medicine

The Graduate School, Yonsei University

DNAJC14 rescues the pathology of misfolded pendrin

Hyeji Choi

Department of Medicine

The Graduate School, Yonsei University

DNAJC14 rescues the pathology of misfolded pendrin

Directed by Professor Jinsei Jung

The Master's Thesis
submitted to the Department of Medicine,
the Graduate School of Yonsei University
in partial fulfillment of the requirements for the degree
of Master of Medical Science

Hyeji Choi

June 2019

This certifies that the Master's Thesis
of Hyeji Choi is approved.

_____

Thesis Supervisor: Jinsei Jung

_____

Thesis Committee Member#1: Jinwoong Bok

_____

Thesis Committee Member#2: Heon Yung Gee

The Graduate School
Yonsei University

June 2019

TABLE OF CONTENTS

LIST OF FIGURES

LIST OF TABLES

ABSTRACT

DNAJC14 rescues the pathology of misfolded pendrin

Hyeji Choi

Department of Medicine

The Graduate School, Yonsei University

(Directed by Professor Jinsei Jung)

In East Asia, the most prevalent mutation in *SLC26A4*/Pendrin, H723R (His723Arg), causes protein folding defect in pendrin, resulting in an autosomal recessive type of genetic hearing loss (DFNB4). There is no curative treatment for hearing loss caused by H723R mutation. The aim of the current study was to rescue H723R-pendrin expression and activity by the activation of DNAJC14 chaperonin through Flavivirus inoculation or overexpression of DNAJC14. We found that toxin-attenuated Japanese encephalitis virus (JEV), which is a Flavivirus, rescued surface expression and anion exchange activity of H723R-pendrin, in vitro. We established a human H723R-pendrin transgenic mouse model (hH723R Tg) with a mouse PDS knock-out background, that only expresses human H723R-pendrin in the inner ear (determined by Pax2-cre), which mimics human DFNB4. When hH723R Tg was crossed with DNAJC14 overexpressed mice, cochlear hydrops was reduced, expression of pendrin in the

endolymphatic duct was increased, and outer hair cells in the cochlea were more preserved, compared to human H723R Tg. Furthermore, with DNAJC14 overexpression, stria vascularis and spiral ligaments were thicker and K^+ channel *KCNJ10* expression contributing to endocochlear potential generation was more abundant. It can be concluded that DNAJC14 rescues the pathology of misfolding in H723R-pendrin and may be a potential therapeutic target for genetic hearing loss.

Key words: DNAJC14, Chaperonin, Hearing loss, Pendrin, Flavivirus

DNAJC14 rescues the pathology of misfolded pendrin

Hyeji Choi

Department of Medicine

The Graduate School, Yonsei University

(Directed by Professor Jinsei Jung)

I. INTRODUCTION

Pendrin encoded by *SLC26A4*/Pendrin is an anion exchanger in the inner ear.[1-3] Mutations in *SLC26A4*/Pendrin cause non-syndromic, autosomal recessive hearing loss (DFNB4), which is the most common cause of congenital deafness in East and South Asia.[4-9] In Korea, the carrier frequency of *SLC26A4*/Pendrin is almost 1 in 75.[5] Sensorineural hearing loss is congenital, fluctuating, progressive, and severe-to-profound.[10] Vestibular functions are also impaired, which has been linked to hearing loss in patients with DFNB4.[11] Because hearing loss in patients with DFNB4 is congenital and severe, most patients undergo cochlear implantation and require hearing rehabilitation. Residual hearing is often observed at an early age, thus there are several years to remedy or prevent hearing loss during the early stages of the disease.[12]

Unfortunately, there is no curative treatment for sensorineural hearing loss in DFNB4.

Of the *SLC26A4*/Pendrin mutations, p.H723R (His723Arg) is the most common pathogenic mutation in Korea and Japan.[13,14] The pathomechanisms of H723R are related to protein misfolding, retention in the endoplasmic reticulum (ER), and degradation by the ER-associated degradation (ERAD) pathway.[15,16] Recently, it has been reported that misfolded proteins can be expressed on the cellular surface via an unconventional trafficking pathway, which is a Golgi-bypassing trafficking on ER stress.[16-18] For instance, H723R pendrin can be rescued to the cell surface via the unconventional trafficking pathway, mediated by heat shock 70 kDa protein (Hsp70) and its co-chaperone DNAJC14. Hsp70 and DNAJC14 interact with H723R pendrin and retrieve the misfolded pendrin from the ERAD and deliver it to the cell surface.[16]

DNAJC14 is an ER chaperonin and it modulates both the cell-surface trafficking of dopamine D1 receptors and the complex-mediated lysosomal trafficking of SNARE.[19,20] Interestingly, DNAJC14 modulates Flaviviridae family RNA replication when viruses are infected in mammalian cells.[21] DNAJC14 is activated by Flavivirus infection and recruited to the virus replication complex and involved in viral replication on the ER membranes by affecting viral polyprotein processing through promoting protein folding.[21-23] This phenomenon is highly reminiscent of the unconventional trafficking of H723R pendrin via Hsp70/DNAJC14 machinery in terms of protein folding and trafficking from ER to the cell surface. Therefore, in the current study, we investigated whether treatment with Flavivirus, such as yellow fever virus or Japanese encephalitis virus (JEV), activates Hsp70/DNAJC14 machinery, enhances the unconventional trafficking of H723R pendrin, and subsequently rescues the function of pendrin. Furthermore, we investigated the effect of enhanced DNAJC14 on the change of inner ear histology and auditory function in H723R-pendrin transgenic mice.

II. MATERIALS AND METHODS

1. Cell culture, transfection, and treatment

PANC-1 cells were maintained in Dulbecco's Modified Eagle's Medium-HG (Lonza, Walkersville, MD, USA) supplemented with 10% fetal bovine serum (FBS) and penicillin (50 IU/ml)/streptomycin (50 ug/ml) at 37℃ with 5% CO_2. Expression plasmids for WT- and H723R-pendrin were subcloned into pCMV-Flag plasmids (Clontech, Palo Alto, CA, USA). To establish PANC-1 stable cells expressing WT-pendrin or H723R-pendrin, transfection of each plasmid into PANC-1 cells using Lipofectamine 2000 reagent (Invitrogen) was performed. Puromycin was used to select the transfected cells during 10 passages.

2. Chemicals and antibodies

Japanese encephalitis virus, Beijing-1 strain propagated in a mosquito cell line C6/36 was kindly supplied by Dr. SK Eo (Chonbuk University, Iksan).[24] Virus stocks were titrated using a conventional plaque assay and stored in aliquots at -80℃ until use. Anti-Flag antibody (F3165) was purchased from Sigma-Aldrich (MO, USA). Anti-DNAJC14 antibody (ab121535) was purchased from Abcam (Cambridge, UK). Anti-β-actin antibody (sc-47778) was purchased from Santa Cruz Biotechnology (Santa Cruz, CA, USA), and the anti-KCNJ10 (Kir4.1, Kir1.2) antibody (APC-035) was purchased from Almone Labs (Jerusalem, Israel).

3. Surface biotinylation assay

Surface proteins were biotinylated with sulfo-NHS-SS-biotin (Pierce) for 30 min before cell lysis. Cells were washed with quenching buffer containing 1% bovine serum albumin (BSA) and then washed three times with phosphate-buffered saline (PBS). Cell lysis was performed with lysis buffer containing 50 mM Tris-HCl (pH 8.0), 150 mM NaCl, 1% (v/v) Triton X-100, and complete protease inhibitor mixture (Roche Applied Science, Mannheim, Germany). Lysates were incubated overnight at 4℃ with 10% NeutrAvidin beads (Pierce). NeutrAvidin-bound biotinylated proteins were centrifuged and washed three times with PBS and then eluted in 2 x sodium dodecyl sulfate (SDS) sample buffer. Protein samples were separated by SDS-polyacrylamide gel electrophoresis (PAGE). Separated proteins were transferred to a nitrocellulose membrane and blotted with appropriate primary and secondary antibodies. Protein bands were detected by enhanced chemiluminescence.[16]

4. Measurement of pH_i and Cl^-/HCO_3^- exchange activity

Measurements of pH-sensitive fluorescent probe 2´,7´-bis-(2-carboxyethyl)-5-(and-6)-carboxyfluorescein (BCECF) was performed in PANC-1 cells transiently transfected WT-pendrin or H723R-pendrin. After JEV treatment for 24 hours, PANC-1 cells were incubated with 2 mM BCECF acetoxy-methylester for 15 min and then perfused with a HCO_3^- buffered solution (120 NaCl, 5 KCl, 1 $MgCl_2$, 1 $CaCl_2$, 10 D-glucose, 5 HEPES and 25 $NaHCO_3$ in mmol l^{-1}, pH 7.4). Next, BCECF fluorescence was recorded on a recording setup (Delta Ram; PTI Inc., Edison, New Jersey, USA) at the excitation wavelengths of 490 and 440 nm at a

resolution of 2/ s^{-1}. Cl^-/HCO_3^- exchange activities were estimated from the initial rate of pH increase as a result of Cl^- removal in the HCO_3^- containing buffer (25 mM HCO_3^- with 5% CO_2).[16]

5. Immunocytochemistry

The PANC-1 cells were cultured on coverslips. Cells were permeabilized by incubation in cold ethanol and acetone (1:1) at 20℃ for 8 minutes. For nonspecific binding site blocking, cells were blocked by incubation with blocking media (0.2 ml PBS containing 5% normal donkey serum, 1% BSA and 0.1% gelatin, and 0.001% NaAzide) at room temperature (RT) for 1 hour. Cells were stained by incubating with appropriate primary and secondary antibodies and viewed under LSM780 confocal microscope (Zeiss Laboratories, Jena, Germany).

6. Construction of H723R mouse

A mouse pendrin H723R knock-in mouse model was generated by Macrogen Inc. (Seoul, Korea) using a homologous recombineering approach, as previously reported.[25] The c.2168A>G mutation in exon19 was applied to H723R-PDS mice. Genotype sequencing was performed with sense primer 5' AGAACCTGAGATGGGGATTCATG 3' and anti-sense primer 5' AGCAAATGCCACATCCGTCAG 3' (size of amplicons: WT: 842 bp, Knock-in: 2126 bp).

A human pendrin H723R transgenic mouse model was established with a Cre-inducible system, where a LoxP-STOP-LoxP sequence from pBigT terminating transcription was subcloned into the EcoRI site of a pCA GGS vector, and cDNA fragment encoding human *SLC26A4* (WT or c.2139G>A) was subsequently ligated using XhoI and NotI sites. Transgene expression in HEK293T cells was confirmed with CMV-Cre plasmid expression. Then the linearized transgene construct was microinjected into pronuclear-stage mouse embryos (C57BL/6N) and transferred to pseudopregnant mice. One transgenic founder mouse harboring human *SLC26A4* (WT or c.2139G>A) was identified by PCR amplification of tail genomic DNA and established through germline transmission. Passage-three human PDS transgenic mice were mated with mouse PDS knock-out mice (kindly gifted by Prof. Sung Huhn Kim) to eliminate mouse pendrin. Next, human PDS Tg(+); mouse PDS (-/-) mice were mated with Pax2-Cre (+) mice [Tg(Pax2-cre)1Akg/Mmnc (Stock: MMRRC no. 010569), kindly gifted by Prof. Jinwoong Bok] to generate Pax2-specific expression of human PDS without mouse PDS. The final mice genotype used for the experiments was human PDS Tg(+)/Pax2-Cre(+); mouse PDS(-/-), where only human pendrin (WT or H723R), but no mouse pendrin, is expressed in the inner ear. Genotyping for human PDS Tg, Pax2-Cre, and mouse PDS KO was performed with the following specific primers: human PDS Tg, Fwd-AACCATGTTCATGCCTTCTTC and Rev-CTAAAGCGC ATGCTCCAGA (amplicon size: 226 bp); Pax2-Cre, Fwd-GCCTGCATTACCGGTCGATGCAACGA and Rev- GTGGCAGATGGCGCG GCAACACCATT (amplicon size: 700 bp); and PDS KO, Fwd-TGCCGATTTCATCGCTGG, Rev1- GCATTGTAGTTCTTTTCCAAGTTGG, and Rev2- GGGTGCGGAGAAAGAGGTAATG (WT: 287 bp and KO: 243 bp).

7. Inner ear western blotting

Mouse inner ears were dissected from approximately 4-to-5-week-old mice for each mouse genotype group. Ear tissue samples were chopped and mashed in lysis buffer. After centrifugation of the lysates, the supernatant lysates were identical to those in the immunoblotting procedure described above.

8. Inner ear histology studies

Tissue samples from the inner ear of mice were fixed in 4% paraformaldehyde (PFA) at 4℃, then washed twice with PBS. Specimens were decalcified in 25% EDTA/PBS for 24 hours. Tissue samples were dehydrated and embedded in paraffin for histological study. Samples were then cut into segments with organ of Corti and permeablized with 0.1% Triton X-100 for whole-mount immunostaining. Paraffin blocks were sectioned into 5 μm using a microtome (Leica Biosystems). Tissue sections were subjected to hematoxylin and eosin (H&E) staining, and immunostaining. Tissue samples stained with H&E were examined using a light microscope. For immunostaining, paraffin sections were deparaffinized with xylene, ethanol, and PBS. For antigen-retrieval, paraffin sections were incubated in sodium citrate at 95℃ for 5 minutes, and then blocked in 10% normal donkey serum (NDS) for 1 hour at RT. Tissue samples were incubated overnight with target-specific primary antibody at 4℃. Samples were then washed and incubated for 1 hour at RT with appropriate secondary antibody. Finally, the samples were washed, and mounted with mounting solution (Sigma-Aldrich, St. Louis, MO, USA). All images of immunostaining were obtained using a confocal microscope LSM780 (Zeiss Laboratories, Jena, Germany).

9. Statistical analysis

The results of multiple experiments are presented as the means ± s.e.m. Statistical comparisons were performed using an analysis of variance (ANOVA) followed by the Bonferroni multiple comparison test, where appropriate. $p<0.05$ was considered statistically significant.

Table 1. Antibodies used in this study.

Name	Catalog number (Manufacturer)	Dilution (Use)
Primary Antibody		
anti-pendrin	sc-23779 (Santa Cruz)	1:1000(WB)
anti-HA-probe	sc-7392 (Santa Cruz)	1:1000(WB)
anti-aldolase	sc-12059 (Santa Cruz)	1:1000(WB)
anti-β-actin	sc-47778 (Santa Cruz)	1:2000(WB)
anti-Flag	F3165 (Sigma-Aldrich)	1:2000(WB), 1:100(IF)
anti-phalloidin FITC	P5282 (Sigma-Aldrich)	1:200(IF)
anti-Hsc70	ab19136 (Abcam)	1:1000(WB)
anti-DNAJC14	ab121535 (Abcam)	1:1000(WB), 1:200(IF)
anti-pendrin	2-hR2 (ABfrontier)	1:1000(WB)
anti-KCNJ10	APC-035 (Alomone Labs)	1:100(IF)
anti-DAPI	D1306 (Thermo)	1:5000(ICC), 1:10000(IHC)
Secondary Antibody		
anti-mouse, HRP conjugated	G-21040 (Thermo)	1:1000(WB)
anti-rabbit, HRP conjugated	32460 (Thermo)	1:1000(WB)
Alexa 488, anti-mouse	A11001 (Invitrogen)	1:1000(IF)
Alexa 488, anti-rabbit	A11008 (Invitrogen)	1:1000(IF)
Alexa 568, anti-rabbit	A11036 (Invitrogen)	1:1000(IF)

WB, western blotting; IF, immunofluorescence; ICC, immunocytochemistry; IHC, immunohistochemistry

III. RESULTS

1. Flavivirus rescues the expression and function of H723R-pendrin

It has been reported that H723R-pendrin has a folding defect and overexpression of DNAJC14 rescues H723R-pendin expression.[16] In the current study, we observed that the surface expression of H723R-pendrin was increased in the DNAJC14-depdendent condition (Fig. 1). Research has shown that Flavivirus, such as JEV, uses DNAJC14 host chaperonin and activates exocytosis of the virus and related proteins to the extracellular surface.[21] Thus, we hypothesized that treatment with JEV could rescue the expression of H723R-pendrin. When stable PANC-1 cells expressing human H723R-pendrin were treated with toxin-attenuated JEV, the surface expression of H723R-pendrin was robustly increased while the levels of H723R-pendrin and DNAJC14 in lysate were not changed. This indicates that the trafficking efficiency of H723R-pendrin to the surface membrane was improved (Fig. 2).

Next, we investigated the anion exchange activity of pendrin when it was treated with JEV. We measured the slope of the pH-sensitive BCECF fluorescence curve when extracellular solution was changed from 150 mM Cl^- to 0 mM Cl^-, then the influx of extracellular HCO_3^- occurred, and pH subsequently increased.[14] Strong Cl^-/HCO_3^- exchange activity was elicited by transfection with WT-pendrin, but not H723R-pendrin. Notably, the compromised anion exchange activity (Cl^-/HCO_3^-) of H723R-pendrin was significantly increased by treatment with JEV (Fig. 3). We also observed, via immunostaining, that H723R-pendrin was restricted in ER while WT-pendrin was well expressed on the cellular surface. With variable amounts of JEV, the cell surface fraction of H723R-pendirn was significantly increased (Fig. 4).

Taken together, these results indicate that JEV treatment, which may induce DNAJC14 activation, increases cell surface expression of H723R-pendrin as well as anion exchange activity of H72R-pendrin.

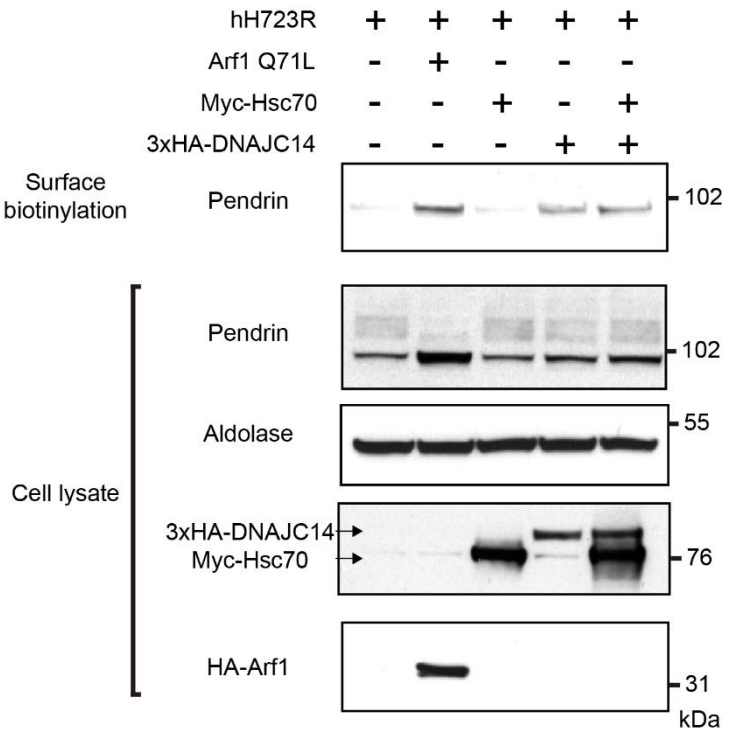

Figure 1. DNAJC14 is increased cell-surface H723R-pendrin expression. Surface biotinylation assays were performed in PANC-1 cells expressing H723R-pendrin. Blockade of ER-to-Golgi traffic by overexpression of Arf1-Q71L induced cell-surface expression of core-glycosylated H723R-pendrin. Overexpression of DNAJC14 (3xHA tagged) alone or with Hsc70 (Myc-tagged) induced cell-surface expression of core-glycosylated H723R-pendrin in PANC-1 cells.

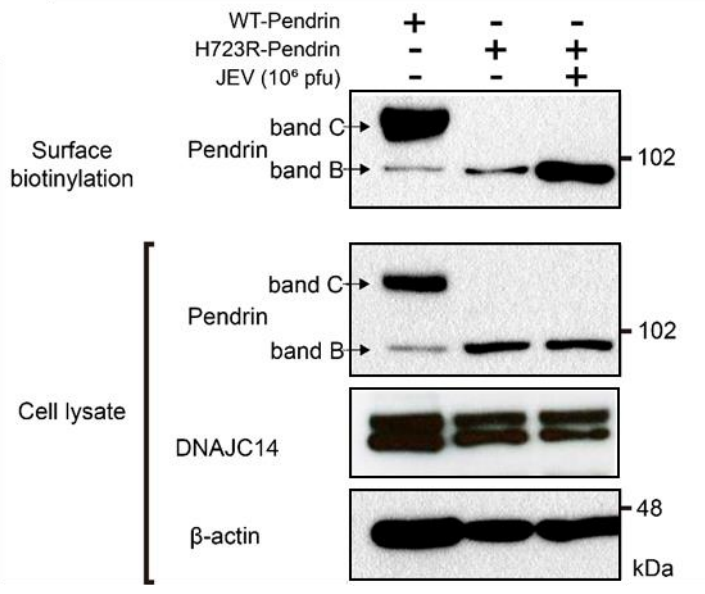

Figure 2. Expression of unconventional cell-surface H723R mutant pendrin increased by JEV. Surface biotinylation assay was performed in PANC-1 cells transfected with plasmids encoding WT- and H723R-pendrin, after treatment with Japanese Encephalitis Virus (JEV). Band B: ER core-glycosylated immature pendrin, band C: fully glycosylated mature pendrin. First lane is positive control cell, the band C form of WT-pendrin was expressed on the cell surface. Second lane is negative control cell, cell-surface band C form of H723R-pendrin was not expressed, band B form was weakly expressed. Last lane is JEV treated cell, JEV induced cell-surface expression of band B form H723R-pendrin.

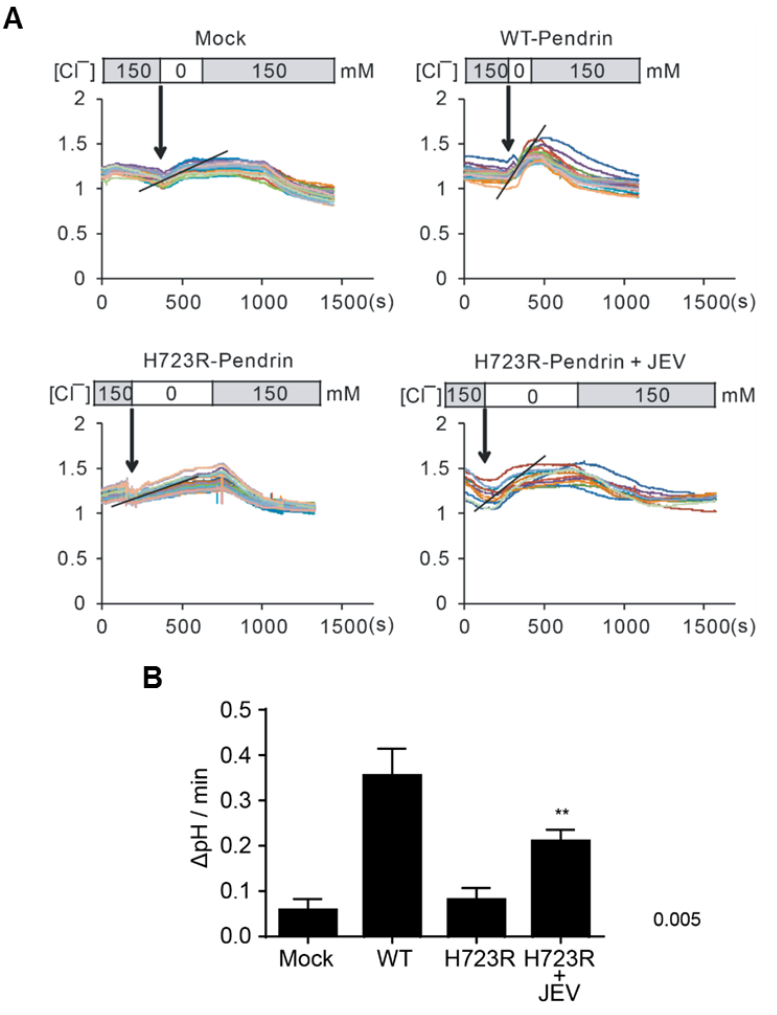

Figure 3. Rescue of anion exchange activity of H723R mutant pendrin by JEV. (A) Cl^-/HCO_3^- exchange activity was measured by recording pH-sensitive fluorescent probe BCECF in PANC-1 mock cell, WT- and H723R- pendrin stable cells, as detailed in Methods. The quantitation of multiple experiments is depicted in (B). The Cl^-/HCO_3^- exchange activity was significantly increased in p.H723R-pendrin treated JEV.

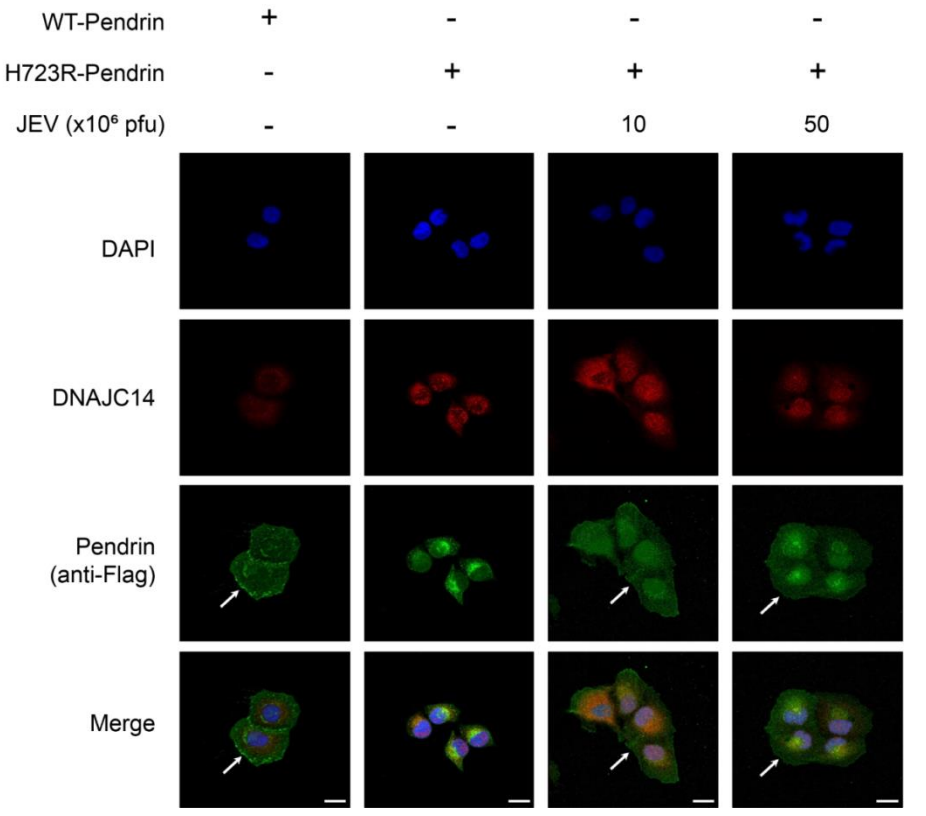

Figure 4. JEV restores the expression of cell-surface H723R-pendrin in immunostainings. Expression of cell-surface pendrin was examined in PANC-1 cells. Cells were stained for pendrin and co-stained for DNAJC14. Nuclei were counterstained with 4’,6-diamidino-2-phenylindole(DAPI). Scale bar, 20 μm.

2. Generation of H723R mouse model mimicking deafness in DFNB4

We established a H723R mouse model with deafness. First, we developed a H723R knock-in mouse. However, the hearing function was normal and there was no abnormality of the inner ear, which is consistent with a previous report.[25] Thus, we developed a human H723R (hH723R) transgenic mice with mouse PDS (mPDS) homozygous knock-out background. We designed a hH723R-flanked transgene (Fig. 5A) and inoculated embryos of C57/B6 mice with it. We then crossed with Pax2-Cre mice to develop mice with inner ear- and kidney-specific expression of hH723R. Next, we crossed hH723R transgenic (Tg) mice with mPDS(-/-) mice which only expressed hH723R (but no mouse pendrin) in the inner ear and kidney (Fig. 5A). For positive control, we also developed wild type (WT)-pendrin Tg (hPDS Tg) mice. In western blot, we observed ectopic expression of WT-pendrin in the kidney and cochlea, but not the liver or intestine (Fig. 5B, left panel). We identified H723R-pendrin in the cochlea of hH723R Tg mice (Fig. 5B, right panel).

Auditory brainstem response (ABR) experiments, demonstrated that hH723R Tg mice showed deafness, mimicking DFNB4 in human; while hPDS Tg mice showed normal hearing (Fig. 5C). Cochlea histological investigation showed that cochlear hydrops was present in both mPDS(-/-) and hH723R Tg(+); mPDS(-/-) mice, but not in hPDS Tg(+); mPDS(-/-), where ectopic WT-pendrin was ubiquitously expressed (Fig. 5D). Whole mount images of cochlear hair cells, showed that outer and inner hair cells were more preserved in hH723R Tg(+); mPDS(-/-) than mPDS(-/-). This demonstrates that ectopic expression of hH723R in the inner ear is minimally helpful to maintain cochlear structure and function (Fig. 5E). Taken together, these results demonstrate that hH723R Tg mice mimic human pathology in DFNB4, such as deafness.

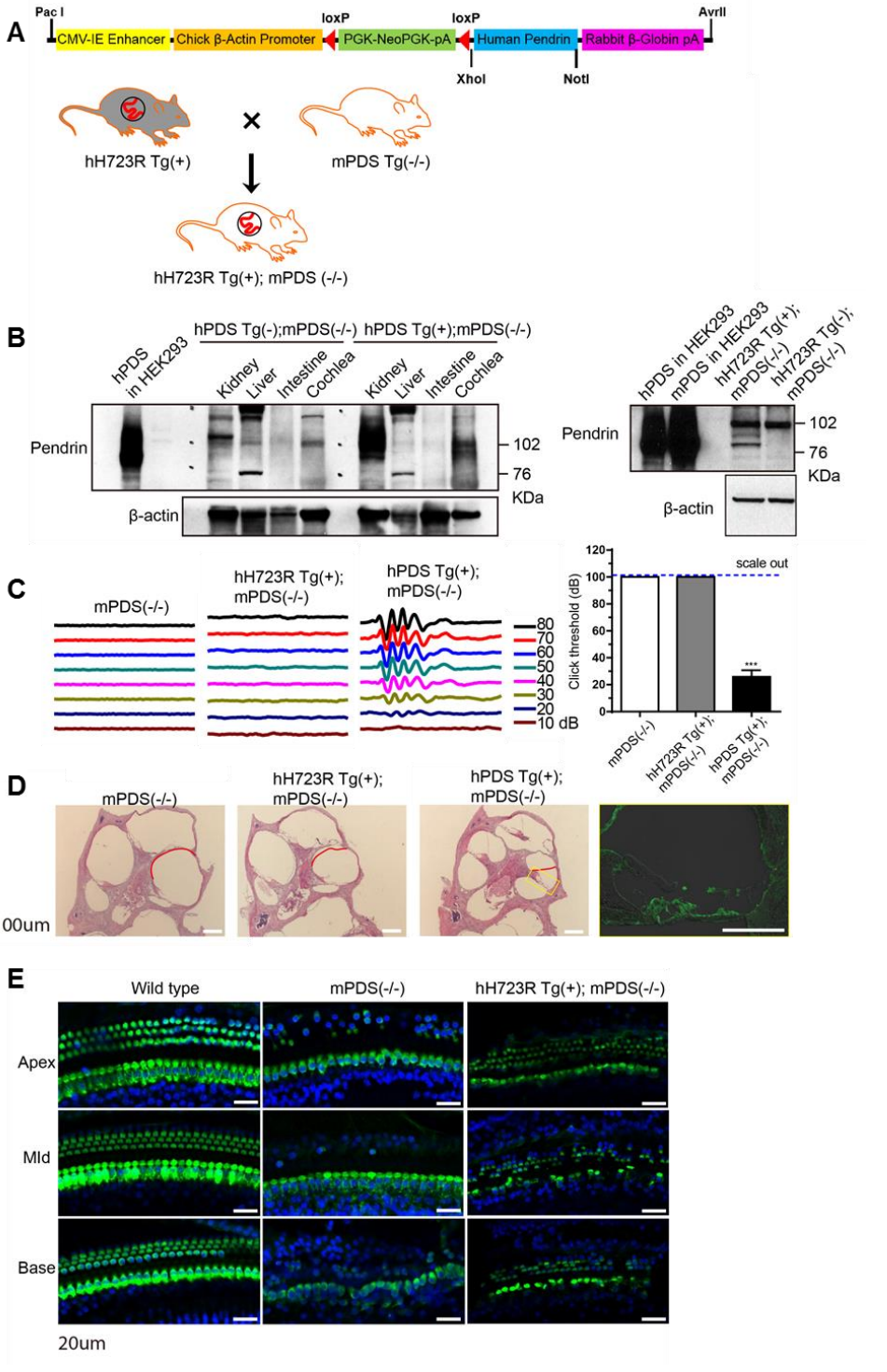

Figure 5. Generation of H723R-pendrin mouse model mimicking deafness in DFNB4. (A) Construct of human H723R PDS (Pendrin) transgene in pCB vector backbone. Wild type or H723R PDS gene is Cre-inducible. hH723R transgenic mouse [Tg(+)] crossed with mouse pendrin knock-out mouse [mPDS Tg(-/-)] to generate hH723R Tg(+); mPDS(-/-), expressing only ectopic human H723R-pendrin, without mouse pendrin. To induce transgene expression in the inner ear, this strain was crossed with Pax2-Cre mice. (B) When hPDS (WT) or hH723R Tg(+) mice crossed Pax2-Cre, gene expression was seen in the inner ear and kidney, while the other organs did not have ectopic expression of pendrin. (C) When ABR was performed for mPDS(-/-), hH723R(+); mPDS(-/-), and hPDS Tg(+); mPDS(-/-), mPDS(-/-) and hH723R Tg(+); mPDS(-/-) were deaf, whereas hPDS Tg(+); mPDS(-/-) mice were rescued and had normal hearing function. (D) H&E staining of the inner ear shows that mPDS (-/-) and hH723R Tg(+); mPDS(-/-) had dilatation of scal media, whereas hPDS Tg(+); mPDS(-/-) had normal size of scala media, without endolymphatic hydrops. Immunostinaing of the inner ear revealed ectopic pendrin expression (anti-pendrin antibody, green) in hair cells, supporting cells, inner limbus, lateral wall, and stria vascularis (Pax2-Cre dependent). Scale bar, 20μm. (E) Immunofluorescence images of the organ of Corti labeled with phalloidin (green) and DAPI (blue) in wild-type, mPDS(-/-), and hH723R Tg(+); mPDS(-/-) mice. Outer hair cells survived more in hH723R Tg(+); mPDS(-/-) than mPDS(-/-) mice.

3. DNAJC14 ameliorates the structural degeneration of hH723R Tg mice

We utilized a hH723R Tg mouse model for therapeutic development the pathology of DFNB4 via DNAJC14 activation. For the activation of DNAJC14, we crossed hH723R Tg mice with DNAJC14 overexpressing Tg mice (Fig. 6A). Overexpressed DNAJC14 was identified in the cochlea, and hH723R-pendrin expression was increased in the cochlea (Fig. 6B). Because the hH723R Tg mouse model is dependent on Pax2-cre expression, most of the cochlea tissue was positive for ectopic pendrin (Fig. 6C). In the endolymphatic duct, hH723R-pendrin expression was also increased in hH723R Tg/DNAJC14 Tg mice (Fig. 6D). Histologically, cochlear hydrops was significantly reduced when DNAJC14 was overexpressed in the cochlea (Fig. 7A and B), stria vascularis and spiral ligament in hH723R Tg/DNAJC14 Tg were more preserved and thicker when compared to hH723R only Tg mice (Fig. 7D and E). In addition, degeneration of outer hair cells in hH723R Tg mice was mitigated by the expression of DNAJC14 (Fig. 8). *KCNJ10*, which is important for the generation of endocochlear potential, was more preserved in the stria vascularis with overexpression of DNAJC14 (Fig. 9). For hearing test, we performed auditory brainstem response (Fig. 10). In hH723R/DNAJC14 mice, the threshold of ABR was not rescued. Nevertheless, these results indicate that DNAJC14 ameliorates cochlear degeneration in hH723R Tg mice.

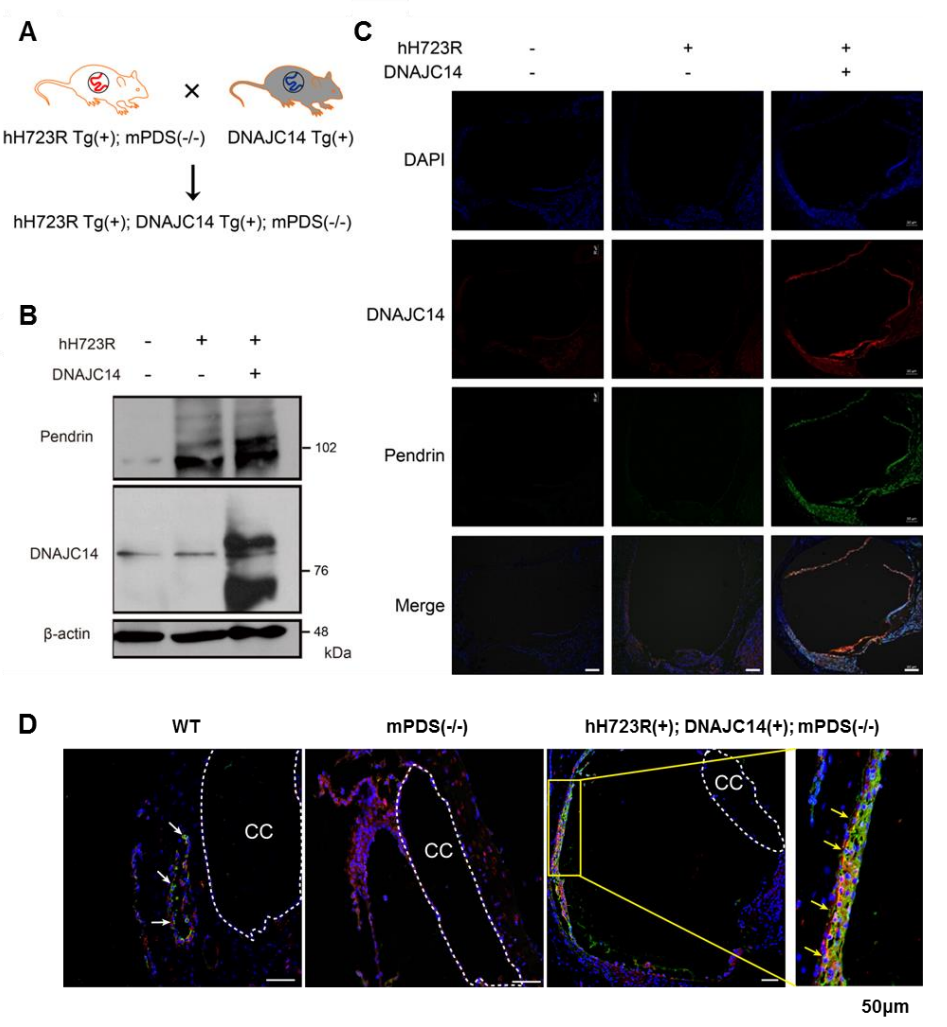

Figure 6. Expression of hH723R Tg/DNAJC14 Tg mice on western blot and immunostaining. (A) hH723R Tg mice were crossed with overexpressed DNAJC14 Tg mice for the activation of DNAJC14 in an established hH723R Tg mice model. (B) Expression of pendrin in the cochlea was increased by overexpressed DNAJC14. Overexpressed DNAJC14 was confirmed in the

cochlea. (C) DNAJC14 expression was identified in hH723R Tg/DNAJC14 Tg mice. Expression of pendrin was increased in most cochlea tissue. (D) Expression of pendrin located in the endolymphatic duct membrane was increased in hH723R Tg/DNAJC14 Tg mice. Staining consisted of immunohistochemistry of DNAJC14 (red), pendrin (green) and DAPI (blue). CC, common cavity; Scale bar, 50 μm.

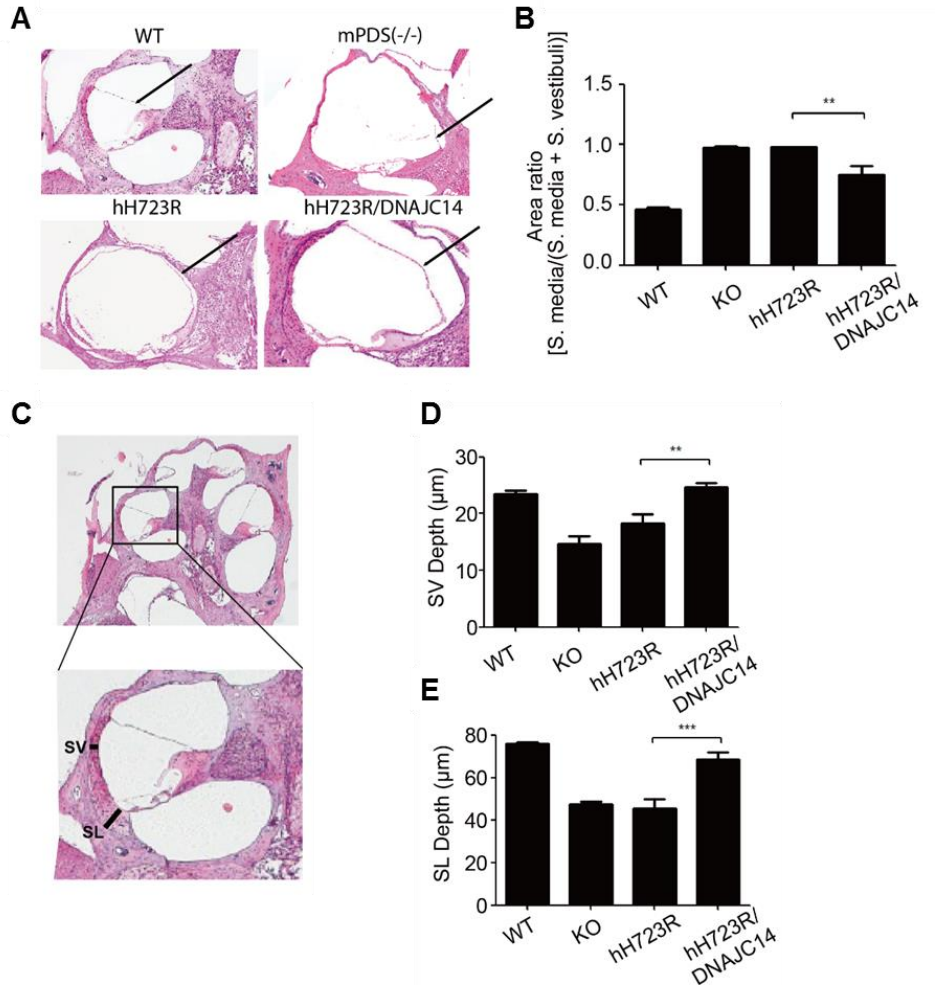

Figure 7. Comparison of cochlear histology in different genotype mice. (A-E) H&E staining from WT, KO, hH723R and hH723R/DNAJC14 mice aged 4-5 weeks. Among the genotype groups, cochlear hydrops of hH723R/DNAJC14 mice was most significantly reduced (B). Stria vascularis (SV) and spiral ligament (SL) depth were thicker in hH723R/DNAJC14 mice than hH723R mice (D,E).

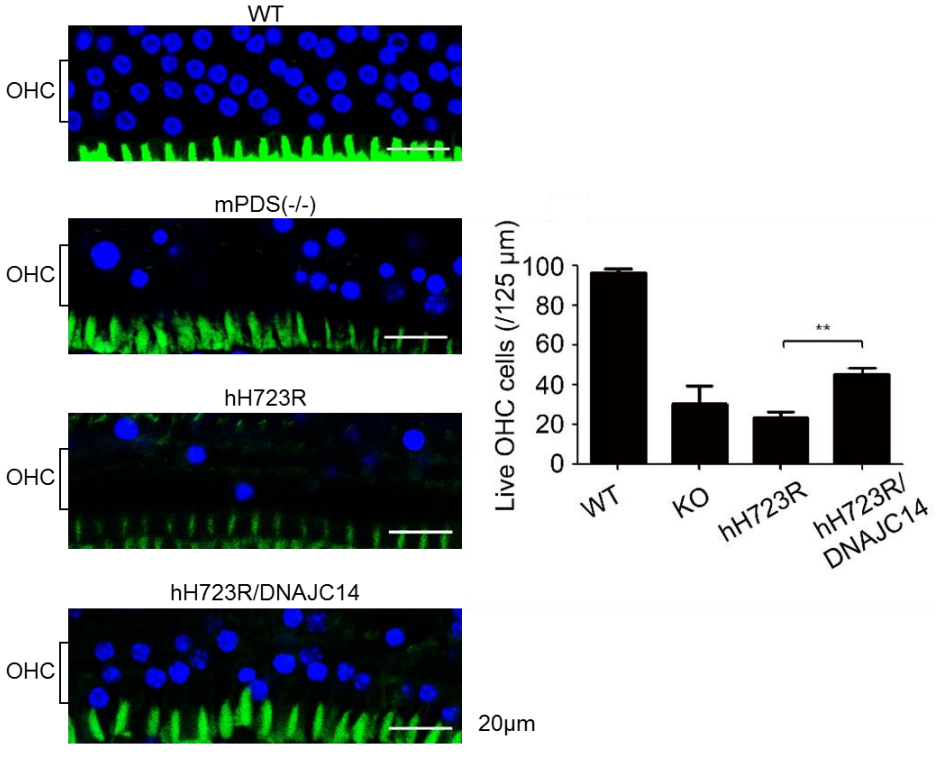

Figure 8. Comparison of outer hair cells in different genotype mice. Whole mount of cochlear outer hair cells (OHC) at the middle turn. The number of OHCs was increased by overexpression of DNAJC14. Immunofluorescence stained with phalloidin (green) and DAPI (blue). Scale bar, 20 μm.

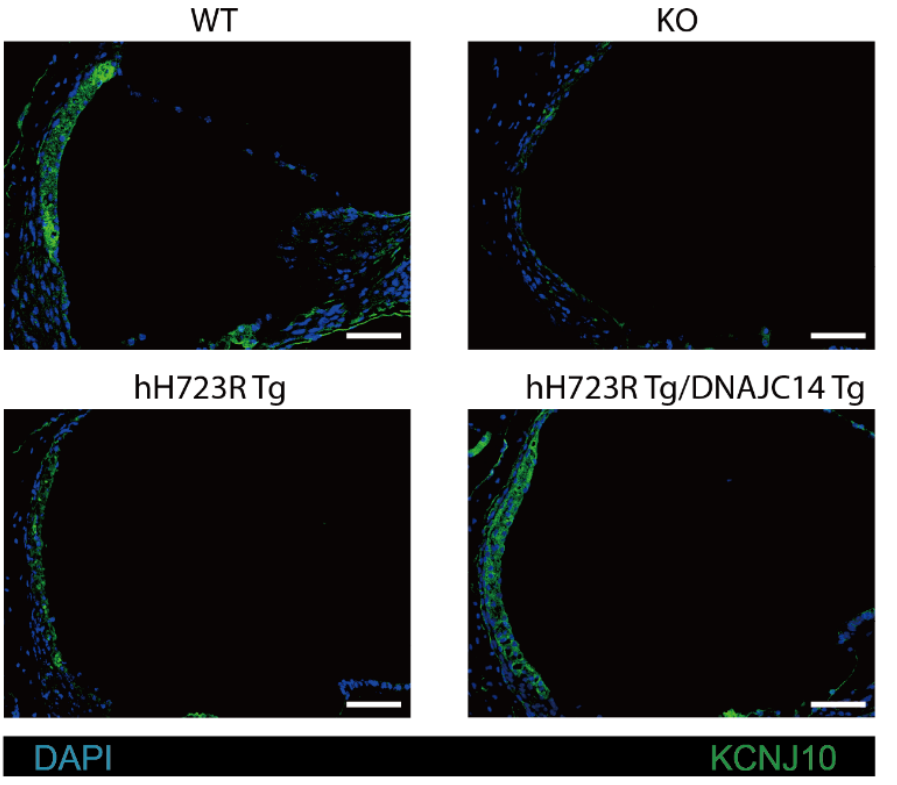

Figure 9. Comparison of *KCNJ10* expression in different genotype mice. *KCNJ10* immunostaining revealed expression of *KCNJ10* was increased in stria vascularis. Implying that endocochlear potential may be partially rescued.

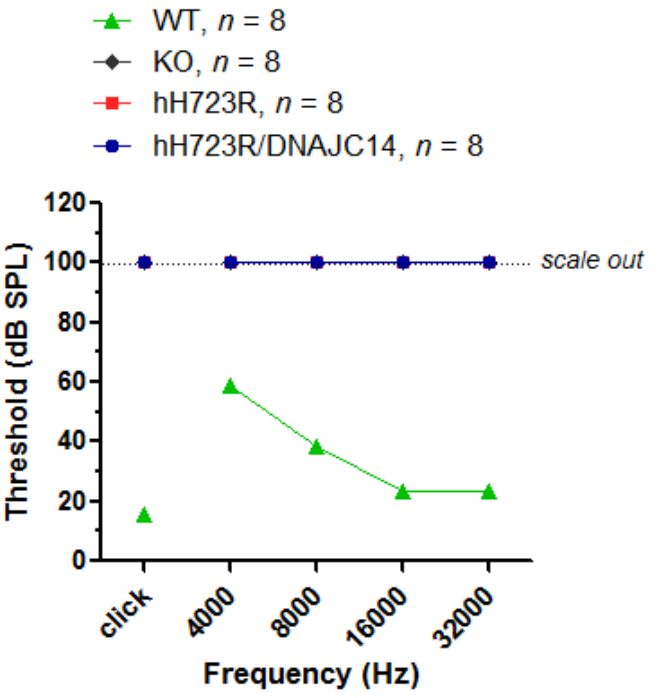

Figure 10. Hearing test of auditory brainstem response (ABR) in different genotype mice. ABR was performed at all frequencies (click, 4, 8, 16, and 32 kHz), WT was normal hearing, whereas KO, hH723R and hH723R/DNAJC14 were deaf (marked as scale out). hH723R/DNAJC14 was not recovered.

IV. DISCUSSION

Genetic hearing loss is very prevalent with an incidence of 1 in 500-1000 children.[26] More than half of congenital hearing loss is caused by genetic variation. However, as yet, there is no clinically curative treatment for patients with genetic hearing loss. Because mutations in *SLC26A4*/Pendrin are the most common cause of hearing loss in East Asia, it is important to develop therapeutics for patients with DFNB4 or Pendred syndrome.

It has been demonstrated that DNAJC14 is the key modulator to rescue misfolded pendrin proteins from ERAD and enhance the expression and function of pendrin.[16] DNAJC14 is an ER chaperonin that plays various physiological roles in mammalian cells, including trafficking of dopamine D1 receptor and lysosome.[19,20] Interestingly, DNAJC14 seems to be utilized in viral RNA replication by infected Flavivirus such as yellow fever virus and JEV.[21,23] Although it is still unclear which functional interaction of DNAJC14 is involved in RNA replication of Flavivirus, it seems to be that DNAJC14 is activated and rearranged on the ER membrane by Flavivirus infection. Because it has been demonstrated that DNAJC14 assists in proper folding of misfolded pendrin and its escape from ER to surface membrane, we reasoned that DNAJC14 activated by Flavivirus infection may also promote protein folding of H723R-penrin. As expected, we found that JEV infection increased cellular surface expression of H723R-pendrin, which is probably related with the promotion of protein folding and rescue H723R-pendrin from ERAD. From this finding, it could be used attenuated Flavivirus such as a vaccine or therapeutic modality for patients with DFNB4 or Pendred syndrome.

Importantly, this study established a mouse model for H723R mutation-related DFNB4. Several animal models with pendrin mutants have

been developed.[27,28] However, it failed to make H723R knock-in mouse model, because there was no human phenotype including hearing loss.[25] In this study, a H723R-pendrin mouse model with deafness was successfully established. In the future, the current model may be used for drug screening, validation, and preclinical trials for hearing preservation drugs focused on protein folding.

This study also demonstrated that overexpression of DNAJC14 in the inner ear ameliorated histological degeneration caused by H723R mutant pendrin. Because *Slc26a4*/pendrin knock-out mice causes enlarged vestibular aqueduct and endolymphatic hydrops, bulging Reissner's membrane in the cochlea due to dilatation of the scala media is typical.[29] In the current study, these finding were also observed in hH723R Tg mice, which leads us to speculate that patients with DFNB4 caused by H723R mutation may also have cochlear hydrops. Importantly, the size of cochlear hydrops in hH723R Tg mice was significantly reduced by DNAJC14 overexpression in the inner ear. Moreover, expression of pendrin was increased in the endolymphatic duct when DNAJC14 was overexpressed. This means that rescued H723R-pendin restores anion exchange (Cl^-/HCO_3^-) activity in the epithelia lining the membranous labyrinth including the scala media, endolyphatic duct, and sac. We found that improving the electrolytic environment in the endolymph prevented structural degeneration of stria vascularis and spiral ligament and protected outer hair cell death. However, hearing was not recovered. Because the protective effect of DNAJC14 on the inner ear histology is limited, DNAJC14 expression is not sufficient to overcome the embryological defect in the H723R mouse model. Thus, the histological anomaly still remained and hair cell degeneration was observed overtime. Nevertheless, it remains promising that the hH723R mouse model was utilized in an *in vivo* screen of small molecules, involved in promoting protein folding.

In summary, we found that activation or overexpression of DNAJC14 increases the surface expression and anion exchange activity of H723R-pendrin.

V. CONCLUSION

The aim of this study was to rescue H723R mutant pendrin, by activation or overexpression of DNAJC14. We found that cell surface expression and anion exchange activity of H723R mutant pendrin was increased by DNAJC14 activation or overexpression. Overexpression of DNAJC14 mice ameliorated structural defects in hH723R Tg mice. These findings may facilitate the development of therapeutics for *SLC26A4*/Pendrin mutation-caused hearing loss.

REFERENCES

1. Everett LA, Glaser B, Beck JC, Idol JR, Buchs A, Heyman M, et al. Pendred syndrome is caused by mutations in a putative sulphate transporter gene (PDS). Nat Genet 1997;17:411-22.
2. Wangemann P, Nakaya K, Wu T, Maganti RJ, Itza EM, Sanneman JD, et al. Loss of cochlear HCO3- secretion causes deafness via endolymphatic acidification and inhibition of Ca2+ reabsorption in a Pendred syndrome mouse model. Am J Physiol Renal Physiol 2007;292:F1345-53.
3. Scott DA, Wang R, Kreman TM, Sheffield VC, Karniski LP. The Pendred syndrome gene encodes a chloride-iodide transport protein. Nat Genet 1999;21:440-3.
4. Park HJ, Lee SJ, Jin HS, Lee JO, Go SH, Jang HS, et al. Genetic basis of hearing loss associated with enlarged vestibular aqueducts in Koreans. Clin Genet 2005;67:160-5.
5. Park HJ, Shaukat S, Liu XZ, Hahn SH, Naz S, Ghosh M, et al. Origins and frequencies of SLC26A4 (PDS) mutations in east and south Asians: global implications for the epidemiology of deafness. J Med Genet 2003;40:242-8.
6. Tsukamoto K, Suzuki H, Harada D, Namba A, Abe S, Usami S. Distribution and frequencies of PDS (SLC26A4) mutations in Pendred syndrome and nonsyndromic hearing loss associated with enlarged vestibular aqueduct: a unique spectrum of mutations in Japanese. Eur J Hum Genet 2003;11:916-22.
7. Wang QJ, Zhao YL, Rao SQ, Guo YF, Yuan H, Zong L, et al. A distinct spectrum of SLC26A4 mutations in patients with enlarged vestibular aqueduct in China. Clin Genet 2007;72:245-54.
8. Wu CC, Yeh TH, Chen PJ, Hsu CJ. Prevalent SLC26A4 mutations in patients with enlarged vestibular aqueduct and/or Mondini dysplasia: a unique spectrum of mutations in Taiwan, including a frequent founder mutation. Laryngoscope 2005;115:1060-4.
9. Dai P, Yuan Y, Huang D, Zhu X, Yu F, Kang D, et al. Molecular etiology of hearing impairment in Inner Mongolia: mutations in SLC26A4 gene and relevant phenotype analysis. J Transl Med 2008;6:74.

10. Pryor SP, Madeo AC, Reynolds JC, Sarlis NJ, Arnos KS, Nance WE, et al. SLC26A4/PDS genotype-phenotype correlation in hearing loss with enlargement of the vestibular aqueduct (EVA): evidence that Pendred syndrome and non-syndromic EVA are distinct clinical and genetic entities. J Med Genet 2005;42:159-65.
11. Jung J, Seo YW, Choi JY, Kim SH. Vestibular function is associated with residual low-frequency hearing loss in patients with bi-allelic mutations in the SLC26A4 gene. Hear Res 2016;335:33-9.
12. Kim BG, Roh KJ, Park AY, Lee SC, Kang BS, Seo YJ, et al. Early deterioration of residual hearing in patients with SLC26A4 mutations. Laryngoscope 2016;126:E286-91.
13. Dossena S, Rodighiero S, Vezzoli V, Nofziger C, Salvioni E, Boccazzi M, et al. Functional characterization of wild-type and mutated pendrin (SLC26A4), the anion transporter involved in Pendred syndrome. J Mol Endocrinol 2009;43:93-103.
14. Lee H, Jung J, Shin J, Song M, Kim S, Lee JH, et al. Correlation between genotype and phenotype in patients with bi-allelic SLC26A4 mutations. Clin Genet 2013; doi:10.1111/cge.12273.
15. Yoon JS, Park HJ, Yoo SY, Namkung W, Jo MJ, Koo SK, et al. Heterogeneity in the processing defect of SLC26A4 mutants. J Med Genet 2008;45:411-9.
16. Jung J, Kim J, Roh SH, Jun I, Sampson RD, Gee HY, et al. The HSP70 co-chaperone DNAJC14 targets misfolded pendrin for unconventional protein secretion. Nat Commun 2016;7:11386.
17. Gee HY, Noh SH, Tang BL, Kim KH, Lee MG. Rescue of DF508-CFTR trafficking via a GRASP-dependent unconventional secretion pathway. Cell 2011;146:746-60.
18. Rabouille C. Pathways of Unconventional Protein Secretion. Trends Cell Biol 2017;27:230-40.
19. Bermak JC, Li M, Bullock C, Zhou QY. Regulation of transport of the dopamine D1 receptor by a new membrane-associated ER protein. Nat Cell Biol 2001;3:492-8.
20. Tchernev VT, Mansfield TA, Giot L, Kumar AM, Nandabalan K, Li Y, et al. The Chediak-Higashi protein interacts with SNARE complex and signal transduction proteins. Mol Med 2002;8:56-64.
21. Yi Z, Sperzel L, Nurnberger C, Bredenbeek PJ, Lubick KJ, Best SM, et al. Identification and characterization of the host protein DNAJC14 as a broadly active flavivirus replication modulator. PLoS Pathog

2011;7:e1001255.

22. Yi Z, Yuan Z, Rice CM, MacDonald MR. Flavivirus replication complex assembly revealed by DNAJC14 functional mapping. J Virol 2012;86:11815-32.
23. Bozzacco L, Yi Z, Andreo U, Conklin CR, Li MM, Rice CM, et al. Chaperone-Assisted Protein Folding Is Critical for Yellow Fever Virus NS3/4A Cleavage and Replication. J Virol 2016;90:3212-28.
24. Choi JY, Kim JH, Patil AM, Kim SB, Uyangaa E, Hossain FMA, et al. Exacerbation of Japanese Encephalitis by CD11chi Dendritic Cell Ablation Is Associated with an Imbalance in Regulatory Foxp3+ and IL-17+CD4+ Th17 Cells and in Ly-6Chi and Ly-6Clo Monocytes. Immune Netw 2017;17:192-200.
25. Lu YC, Wu CC, Yang TH, Lin YH, Yu IS, Lin SW, et al. Differences in the pathogenicity of the p.H723R mutation of the common deafness-associated SLC26A4 gene in humans and mice. PLoS One 2014;8:e64906.
26. Jung J, Lee JS, Cho KJ, Yu S, Yoon JH, Yung Gee H, et al. Genetic Predisposition to Sporadic Congenital Hearing Loss in a Pediatric Population. Sci Rep 2017;7:45973.
27. Lu YC, Wu CC, Shen WS, Yang TH, Yeh TH, Chen PJ, et al. Establishment of a knock-in mouse model with the SLC26A4 c.919-2A>G mutation and characterization of its pathology. PLoS One 2011;6:e22150.
28. Choi BY, Kim HM, Ito T, Lee KY, Li X, Monahan K, et al. Mouse model of enlarged vestibular aqueducts defines temporal requirement of Slc26a4 expression for hearing acquisition. J Clin Invest 2011;121:4516-25.
29. Everett LA, Belyantseva IA, Noben-Trauth K, Cantos R, Chen A, Thakkar SI, et al. Targeted disruption of mouse Pds provides insight about the inner-ear defects encountered in Pendred syndrome. Hum Mol Genet 2001;10:153-61.

ABSTRACT (IN KOREAN)

DNAJC14 샤페로닌 조절에 의한 H723R 돌연변이 펜드린의 발현 및 기능 회복

<지도교수 정 진 세>

연세대학교 대학원 의학과

최 혜 지

유전성 난청은 500 ~ 1000 명의 어린이 중 1 명 꼴로 발생하는 매우 만연한 질병이며, 선천성 난청의 절반 이상이 유전적 변이에 의해 유발된다. 그 중에서도 특히, *SLC26A4*/펜드린 p.H723R(His723Arg) 돌연변이가 동아시아에서 유전성 난청을 일으키는 가장 흔한 원인 변이이고, 이 돌연변이는 단백 접힘 이상을 초래하여 세포막으로 도달하지 못하는 것으로 알려져 있다. 그러나, 아직 유전성 난청 환자들을 위한, 임상적으로 치료 가능한 치료법이 없다. 그래서 본 연구로, H723R 펜드린의 비전형적 단백 수송 경로를 통한 H723R 돌연변이 펜드린이 세포막으로 도달할 수 있도록, Flavivirus 또는, DNAJC14의 과발현을 통한 DNAJC14 조절현상을 이용하여, H723R 돌연변이 펜드린을 교정하고자 하였다.

Flavivirus의 JEV를 treat하여, DNAJC14를 세포주에서 과발현시켜, p.H723R 펜드린의 세포막 발현이 증가하는 것을, surface biotinylation

assay와 immunocytochemistry를 통해 확인하였고, 펜드린의 기능인, anion exchange activity가 향상되는 것을 Cl^-와 HCO_3^- 의 exchange activity를 측정하여 확인하였다.

또한, hH723R 펜드린 마우스 모델에 DNAJC14를 과발현시킨 마우스 모델을 제작하였고, 이를 통해 내이 내 H723R 돌연변이 펜드린에 의한 조직학적 퇴화가 개선되는 것을 확인하였다. 먼저, 난청을 가진 펜드린 knock-out 마우스의 주된 특징인 증가되어 있던 hydrops의 크기가 현저히 줄어드는 것을 H&E를 통해 확인하였고, 청력회복까지는 미치지 못했지만 stria vascularis와 stria ligament의 두께가 증가한 것으로 보아 구조적 퇴화를 막아주는 것을 확인하였고, endolymphatic duct에 hH723R 펜드린의 발현이 증가되어있는 것과 외유모세포의 죽음을 막아주는 것 또한 확인하였다.

결론적으로, 본 연구를 통해 DNAJC14의 활성화 또는 과발현이 H723R 돌연변이 펜드린의 세포막 발현 및 음이온 교환 기능을 증가시킨다는 것을 확인하였고, 나아가 *SLC26A4*/Pendrin 돌연변이에 의한 유전성 난청의 치료제 개발에 대한 해결의 실마리를 찾는데 도움이 될 것으로 생각된다.

핵심되는 말: 드나제이씨14, 샤페로닌, 난청, 펜드린, 플라비바이러스